

## Article

# Gold Provenance in Placers from Pureo Area, Southern Chile Coastal Cordillera, and Their Relationship with Paleozoic Metamorphic Rocks

Pablo Becerra <sup>1,\*</sup> , Pablo Sanchez-Alfaro <sup>1,2</sup>, José Piquer <sup>1</sup>, Gaëlle Plissart <sup>1</sup>, Belén Garroz <sup>1</sup> and Daniela Kunstmann <sup>1</sup>

<sup>1</sup> Instituto de Ciencias de la Tierra, Universidad Austral de Chile, Valdivia 5110566, Chile

<sup>2</sup> Andean Geothermal Center of Excellence (CEGA), Universidad de Chile, Santiago 8370450, Chile

\* Correspondence: pablo.becerra01@alumnos.uach.cl

**Abstract:** Southern Chile placer gold deposits have been known and exploited since Spanish colonial times. Despite this, precise knowledge about their origin is scarce. This work aims to identify possible primary sources of the gold in the Pureo placers by studying the morphological and chemical characteristics of gold particles according to their spatial distribution. The former was determined by measurements and classification under a binocular microscope, allowing us to acquire a set of parameters related to the amount of transport that had affected the samples. The microchemical characteristics were determined by studying gold particles using optical microscopy, scanning electron microscopy (SEM) and electron microprobe (EMPA), where the native gold composition (in terms of major and minor elements) and the suite of mineral inclusions were obtained. The results regarding morphological characteristics suggest a low amount of transport from a primary source (<15 km). Microchemical data from gold particles indicate two compositional sub-populations, distinguished in both native gold composition (<15 Ag wt% with up to 4 Hg wt% and >15 Ag wt% with Hg below 1 wt%) and mineral inclusions (pyrite-galena rich and arsenopyrite rich, respectively), indicating two different primary gold sources. These results suggest a local origin of gold in the Coastal Cordillera, where the possible primary sources are associated with (i) massive sulfide deposits present in Paleozoic–Triassic metamorphic rocks and (ii) hydrothermal deposits associated with more recent Cenozoic intrusive activity. These conclusions have implications for the exploration of new placer deposits and of gold-bearing hypogene deposits (e.g., metamorphosed VMS deposits) in unexplored zones of southern Chile Coastal Cordillera.

**Keywords:** placers; gold; Chile; gold microchemistry; gold morphometry; gold provenance



**Citation:** Becerra, P.; Sanchez-Alfaro, P.; Piquer, J.; Plissart, G.; Garroz, B.; Kunstmann, D. Gold Provenance in Placers from Pureo Area, Southern Chile Coastal Cordillera, and Their Relationship with Paleozoic Metamorphic Rocks. *Minerals* **2022**, *12*, 1147. <https://doi.org/10.3390/min12091147>

Academic Editor: Galina Palyanova

Received: 6 August 2022

Accepted: 7 September 2022

Published: 10 September 2022

**Publisher's Note:** MDPI stays neutral with regard to jurisdictional claims in published maps and institutional affiliations.



**Copyright:** © 2022 by the authors. Licensee MDPI, Basel, Switzerland. This article is an open access article distributed under the terms and conditions of the Creative Commons Attribution (CC BY) license (<https://creativecommons.org/licenses/by/4.0/>).

## 1. Introduction

Placers are the earliest known and worked gold deposits [1]. Their formation is related to the physical transport and concentration of gold particles from primary sources; therefore, their physical and chemical features can be used to trace the original source of gold mineralization. Systematic study of placer gold particles in a variety of geological environments concurs in terms of two key characteristics of placer gold particles related to their provenance. First, particle morphology evolution is considered to be directly related to transport distance [2,3]. The size and shape of gold particles are affected during their transport in a fluvial environment, being gradually flattened and rounded as they are transported [2,4,5]. On the other hand, the microchemical characteristics of particles have been related to the type of primary deposit from which the particles were eroded [6,7], where native gold composition and mineral inclusions are considered the principal characteristics related directly to the conditions of gold formation in the hypogene environment, which are commonly studied by using SEM and EMPA techniques [6,7]. Several works have used these relationships to investigate the provenance of gold particles in placer deposits

worldwide, in terms of their transport distance [3] and the style of primary gold-bearing deposit that originated the particles [8], constituting an exploration tool for unknown primary gold deposits [6].

In southern Chile, placer gold deposits have been known and exploited since Spanish colonial times [9]. Despite this, the source of the gold remains unclear. Previous work about gold particles in southern Chile placers has proposed that a large part of the gold at a regional scale comes from eroded primary deposits in the Andean Principal Cordillera [10]. However, it has also been suggested that some placer deposits in the Coastal Cordillera have a local origin [10,11] that could be related to metamorphic or magmatic-hydrothermal processes in the Paleozoic metamorphic rocks constituting the Coastal Cordillera. The Pureo gold placer area, located in the Coastal Cordillera at  $\sim 39^\circ$  S, offers an opportunity to study the primary sources of gold in southern Chile because: (1) placers are being actively exploited by small-scale artisanal miners, whose mining tunnels allow access to the deposits; and (2) placers are located relatively close ( $<20$  km) to known primary occurrences of gold in metamorphic rocks [12,13]. In this work, we aim to identify possible primary sources of gold for the placer deposits in the Pureo area by studying the morphological and microchemical characteristics of the gold particles according to their spatial distribution in order to identify their relationships with primary source(s) within the metamorphic rocks that constitute this zone of the Coastal Cordillera.

## 2. Geological Background

The Pureo area is located in the southern Chile Coastal Cordillera, a mountain range along the Pacific Coast [13], composed mainly by a heterogeneous unit of Paleozoic-Triassic, highly deformed metamorphic rocks. In the study area, this basement is made by a low T-high P unit, grouped as the Bahía Mansa Metamorphic Complex (BMCC, Figure 1) [14,15], which corresponds to the oldest geological unit in this zone [16]. The BMCC consists of pelitic to semi-pelitic and mafic schists and minor occurrences of serpentinized ultramafic rocks [14,17]. The BMCC is interpreted as a paleo-accretionary prism associated with subduction that was active during the Late Paleozoic, for a period of 50–100 Ma [15].

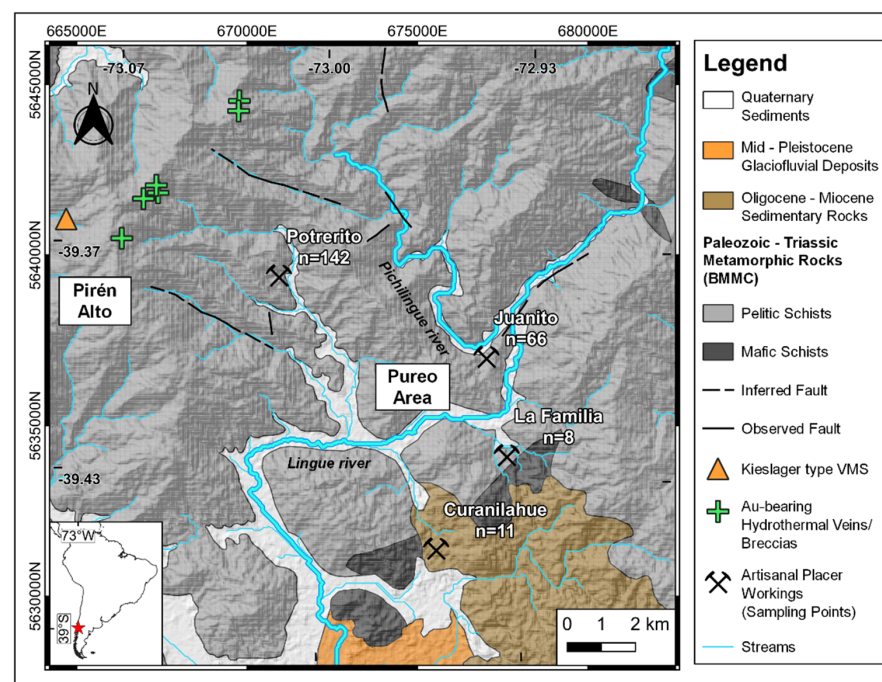


**Figure 1.** Geological map of the Pureo area. Hypogene mineralizations and active placer artisanal workings with the respective samples are shown. BMCC: Bahía Mansa Metamorphic Complex (modified after [12,13,16,18–20]).

Frequent occurrences of mineralized rocks have been reported in this area, corresponding to metamorphosed deposits associated with BMMC rocks, especially small lenses of Kieslager-type massive sulfide (VMS) deposits (Pirén Alto occurrence, Figure 1, [18,21,22]) and associated exhalites as banded iron formations and “coticles” (spessartine-rich metacherts), which are genetically related to a common sub-marine volcanic-exhalative origin [12,21,23]. In addition, occurrences of gold-bearing hydrothermal veins and breccias associated with probable Cenozoic intrusions have been reported (Pirén Alto prospect, Figure 1; [12,13,24,25]). Both occurrences are located to the northwest of the placer deposits (Figure 1). Detailed information about the deposits that host the placers, such as sedimentary facies, spatial extension, or the specific ages of these auriferous gravel deposits in the Pureo area, remains scarce. Despite this, placer locations near the Pureo area at regional scale are hosted in an early Pleistocene unit of glaciofluvial gravel deposits [26], and consequently, the Pureo placers could be related to a similar unit. Although these deposits are considered fossil placers, we refer to them as placers, considering that the term ‘placer’ is commonly used for Cenozoic deposits (e.g., [27]). Auriferous gravels in the Pureo area form old subhorizontal terraces over the main channels of the Pichilingue and Lingue rivers [28] which are currently worked by local artisanal miners. These deposits overlay the BMMC rocks (Figure 2) and are almost exclusively formed by clasts of BMMC lithologies [12]. Gold is irregularly distributed in the gravels, but the highest concentrations are restricted to the first 4–5 m above the bedrock [29].

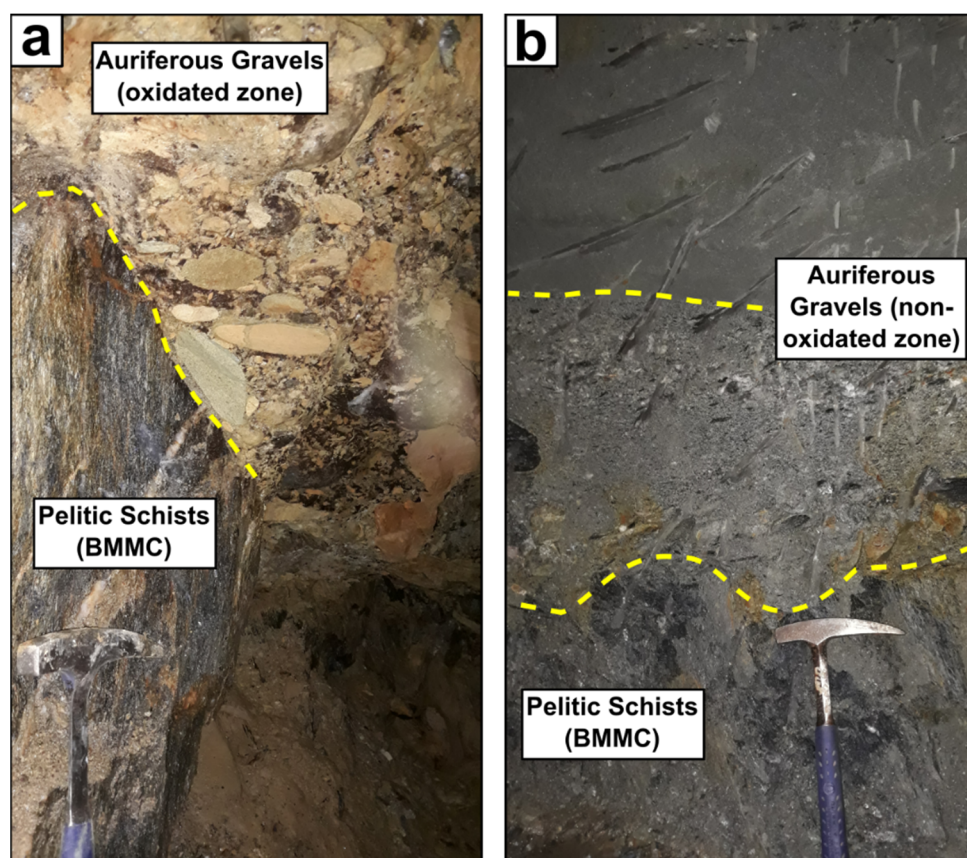


**Figure 2.** Auriferous gravels overlying pelitic schists of BMMC. Photographs from underground workings, following the boundary between gravels and bedrock (pelitic schists) within the terraced deposits. (a) A near-surface oxidated zone of gravels that exhibit reddish colors. (b) Farther surface non-oxidated zone of gravels, exhibiting bluish grey colors. In both locations, sediments for hand-panning were taken immediately above the contact with pelitic schists (above the yellow dashed line).

### 3. Materials and Methods

#### 3.1. Sample Collection

Samples of gold particles were collected manually by hand-panning auriferous gravels from four underground artisanal mines, with the support of local miners (Figure 1). Auriferous gravels were taken in the first 1–2 m above the bedrock. Although these artisanal workings exploit the same gravels, some differences in the oxidation level of the auriferous gravels were observed between them (Figure 2), e.g., in the workings that exploit parts of the deposit close to the surface, the gravels exhibit reddish colors (Curanilahue, Potrerito), while some tunnels that go far away from the surface expose less oxidated zones and exhibit bluish grey colors (Juanito, La Familia). Particles were separated and handpicked under a binocular microscope. A total of 227 particles were recovered. The number of particles obtained for each mine is indicated in Figure 1.

#### 3.2. Morphological Analysis

A morphological analysis of the particles was carried out following the methodology described in [30], which consists of the processing of images of particles taken under an optical microscope using plugins in the *ImageJ* software (version 1.52o) [31]. The output from *ImageJ* consists of the dimensions of each gold particle: length (L), width (W) and thickness (t). Two photographs of perpendicular cross-sections were taken to each group of particles. This information was used to calculate morphological indices which are commonly used in the literature, i.e., the Cailleux Flatness Index [32] and Shilo's Flatness Index [33,34], both of which can quantify the mass redistribution in malleable particles due to progressive hammering during transport in fluvial environments. The CFI and SFI calculations are shown in Equations (1) and (2), respectively:

$$\text{CFI} = (L + W)/2t, \quad (1)$$

$$\text{SFI} = [(L + W)/2t] - 1, \quad (2)$$

Higher CFI and SFI values reflect greater amounts of transport [2–5,32]. Another calculated index was Hofmann's Shape Entropy [35]. Its calculation is shown in Equation (3):

$$\text{HSE} = -[(pL \cdot \ln pL) + (pW \cdot \ln pW) + (pt \cdot \ln pt)]/1.0986, \quad (3)$$

where  $p$  is the proportion of each particle axis (L, W, t) and 1.0986 is the maximum possible relative entropy value for a three-component system [35]. This index reflects the particle evolution from equidimensional shapes to flattened disks due to transport and was used by [36] to quantitatively estimate a model for particle shape-transport distance of gold in Klondike placers. Values of HSE lower than 1 reflect progressive flattening and greater transport [30,36,37].

#### 3.3. Microchemical Analysis

A total of 75 gold particles were mounted in epoxy and polished for microchemical analyses. Polished sections were first observed using a reflected light optical microscope to identify target zones for subsequent analysis. SEM-EDS microanalyses were done with a Zeiss EVO-MC10 SEM, with an accelerating voltage of 20 kV and a working distance of 8 mm, at the Universidad Austral de Chile (UACH) in Valdivia, Chile. These microanalyses allowed us to accurately identify mineral inclusions and chemical zoning inside gold particles. Quantitative EMPA analyses were done in previously selected zones of 19 particles with a Cameca SX50 Electron Microprobe at the Institut Français de Recherche pour L'exploitation de la Mer (IFremer) in Brest, France. Both particle cores and rims were analyzed separately, as they represent the original primary native gold composition [6] and supergene altered composition, respectively [2,38,39]. Selected zones were analyzed for Au, Ag, Hg, Cu, Te, Pt, Pd. Complementarily, a gold grain found as an inclusion in a pyrite from a cotecule clast from Juanito mine was analyzed as it represents a possible

source lithology. EMPA analysis were performed with an accelerating voltage of 20 kV and a beam current of 50 nA with counting times of 30 s for each element at peak and 15 s for background. Estimated detection limits were 0.1 wt% for Au, 0.11 wt% for Ag, 0.02 wt% for Hg, 0.038 wt% for Cu, 0.04 wt% for Te, 0.15 wt% for Pt, and 0.1 wt% for Pd. Punctual analysis, transects and maps were performed in both SEM-EDS and EMPA analysis.

## 4. Results

### 4.1. Particle Morphology

Mean gold particle size values for the Pureo area in terms of length (L), width (W) and thickness (T) were 1.14 mm, 0.78 mm, and 0.38 mm respectively. Gold particle sizes and morphological indexes are shown in Figure 3 for each mine.

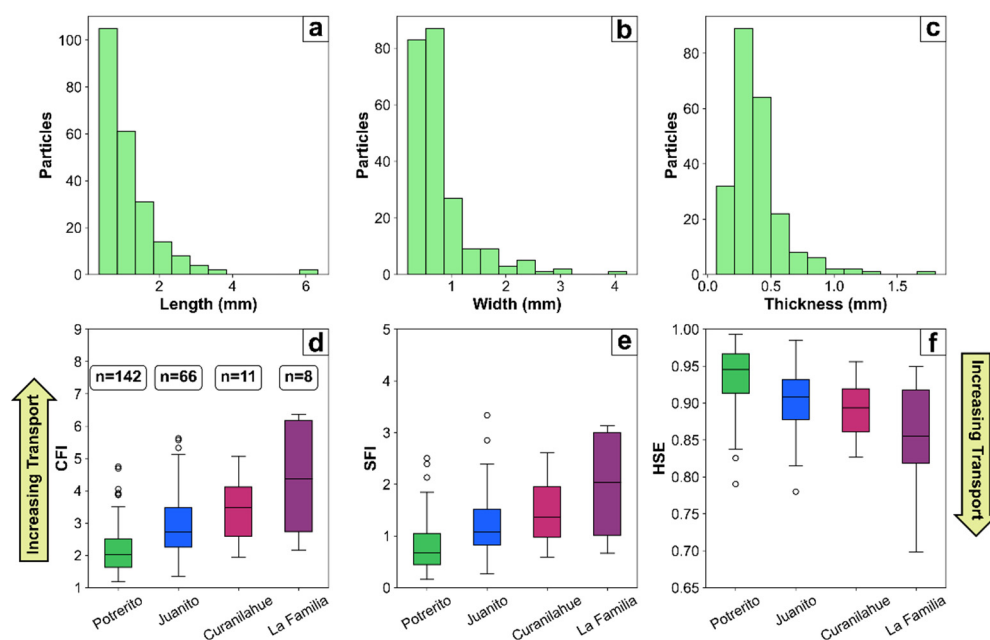


**Figure 3.** Gold particle size and morphological index values obtained in the Pureo area. (a–c) Histograms of particle dimensions (Length (L), Width (W) and Thickness (T)) for all samples. (d–f) Box-plots for morphological index values. Boxes represent inter-quartile range, horizontal line in the boxes represents the median, whiskers extend from the box by 1.5x the inter-quartile range and the white dots represent outlier values that are outside the whiskers. CFI: Cailleux's flatness index, SFI: Shilo's flatness index. Both CFI and SFI increase with increasing transport; HSE: Hofmann's shape entropy. HSE decreases with increasing transport.

Gold particles from Juanito and Potrerito showed the lowest and the most homogeneous morphological index values. The Potrerito particles showed the lowest CFI and SFI values, varying between 1–3 and 0–2 respectively (Figure 3d,e), with the bulk of particles exhibiting HSE values higher than 0.9 (Figure 3f). Particles from Juanito showed similar values, but slightly higher for CFI and SFI, with values varying between 2–4 and 1–3 respectively (Figure 3d,e), and lower HSE values. The Curanilahue and La Familia particles showed a wider range of morphological index values (Figure 3d,e), probably due to the low number of recovered samples. The highest CFI-SFI and lowest HSE values were found in a particle from La Familia. Another characteristic of the Pureo particles is the common observation of accessory minerals conserved in their surfaces, mainly quartz, Fe-oxides and less commonly, pyrite (Figure 4). Particles showing accessory minerals were documented in all the sampled mines.

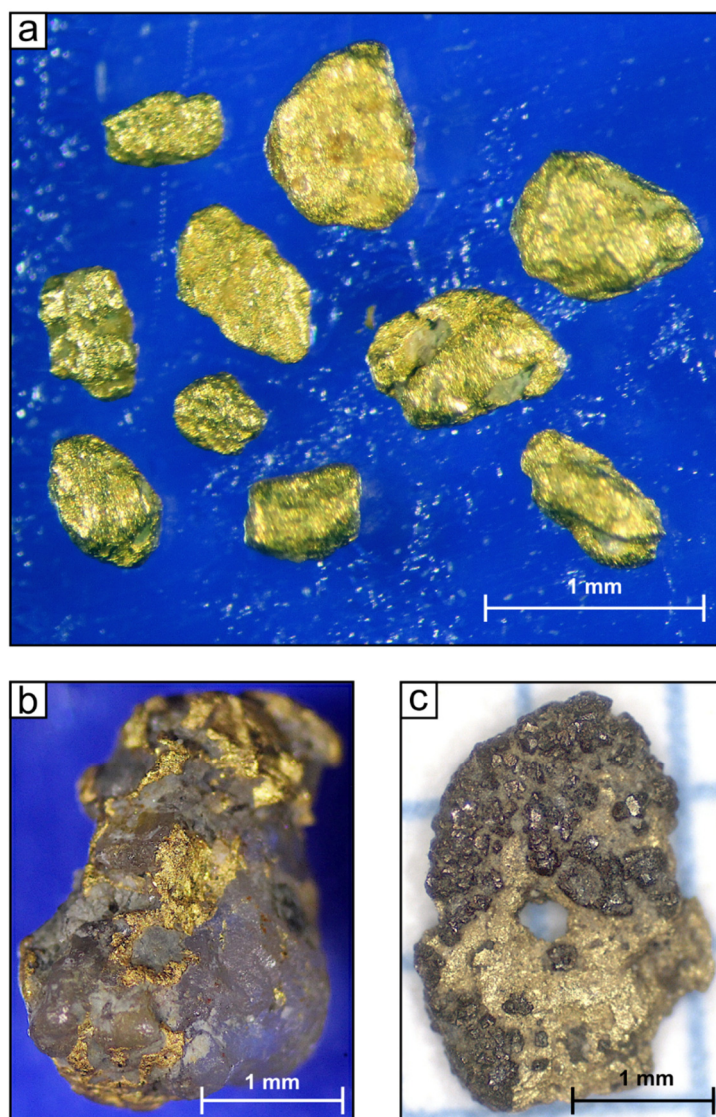


**Figure 4.** Placer gold particles from the Pureo area. (a) Gold particles under binocular microscope. (b) Quartz pebble with inclusions of native gold, which has not been released from its quartz matrix, probably from an eroded vein. (c) Pyrite coverage over particle surface.

#### 4.2. Microchemical Characteristics

##### 4.2.1. Native Gold Composition and Internal Chemical Zonations

A total of 75 gold particles were analyzed using SEM-EDS in order to determine the semi-quantitative native gold composition. Additionally, 19 of them were analyzed in EMPA to determine the quantitative composition. In general, our microchemical results showed that Pureo native gold particles mainly comprised Au and Ag with minor detectable Hg contents ( $>0.02$  wt%) in the particle cores, recorded in all particles analyzed with EMPA. The contents of all other elements, such as Cu, Te, Pt, and Pd, were below the detection limits.

The semi-quantitative silver compositions of the 75 particle cores, as determined by SEM-EDS analyses, are shown in a cumulative frequency plot (Figure 5a), which shows homogeneous curves in the La Familia and Curanilahue particles. Conversely, the Potrerito and Juanito curves show a slope break at around 15 Ag wt% (850‰ Au) (Figure 5a), and therefore, two compositional sub-populations were distinguished in terms of their Ag contents. Quantitative core compositions, as determined by EMPA punctual analyses, varied between 72.9–94.4 wt% Au, 5.7–28.1 wt% Ag and 0.02–4.02 wt% Hg. These compositions

are equivalent to a gold fineness range between 649–955‰ in particle cores. An important observation is that Ag and Hg appear to be slightly inversely correlated (Figure 5b). In other words, the particle cores that showed highest mercury contents were those with the lowest silver contents (<15 Ag wt%).

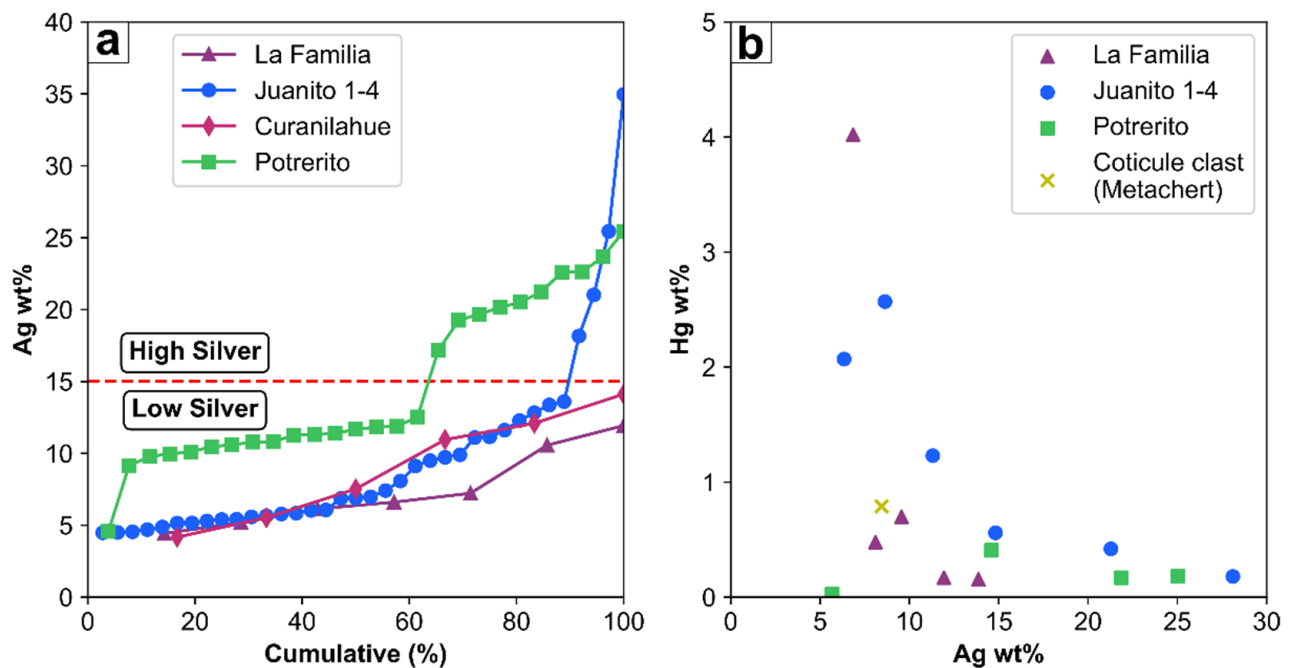


**Figure 5.** Compositions of native gold particle cores determined with SEM-EDS and EMPA analyses. (a) Cumulative frequency plots for semi-quantitative core silver contents obtained with SEM-EDS. (b) Variations in quantitative silver and mercury contents obtained with EMPA. The composition of a gold grain found as a pyrite inclusion in a “coticule” (metachert) clast is shown. Particles with lower silver contents show the highest mercury contents.

Chemical zonations associated with different proportions of native gold components were observed. Ag-Hg-depleted rims (Figure 6a) were the most common zonation found, characterized by a depletion of these elements and an enrichment of Au that develops in the rims and fractures of the particles. Rim zonation is limited by marked and abrupt contact between the two compositions without any transitional zones between the cores and the Ag-Hg-depleted rims (Figure 6a). An estimation of the rim proportion was done by measuring two transects over the particle section analyzed in a BSE image, calculating the proportion of the line segment contained in the rim and its length and averaging them (Figure 7). Rim size was observed to be higher in particles recovered from near surface areas of the auriferous gravel deposit, which present marked oxidation (Figure 7). In contrast, in the particles recovered farther from surface with a lower oxidation, the size of the rim is smaller (Figure 7). The oxidation levels of the gravel deposits were observed in artisanal underground workings as an abrupt change in the deposit color (Figure 2). Although gold particle cores are mostly compositionally homogeneous, some particles showed heterogeneities that occur in the form of irregular or ‘vein-like’ patches with a different composition from that of the surrounding core (Figure 6b). Compositionally heterogeneous cores were observed only in six gold particles from Potrerito that exhibited high silver contents (over 15 Ag wt%).

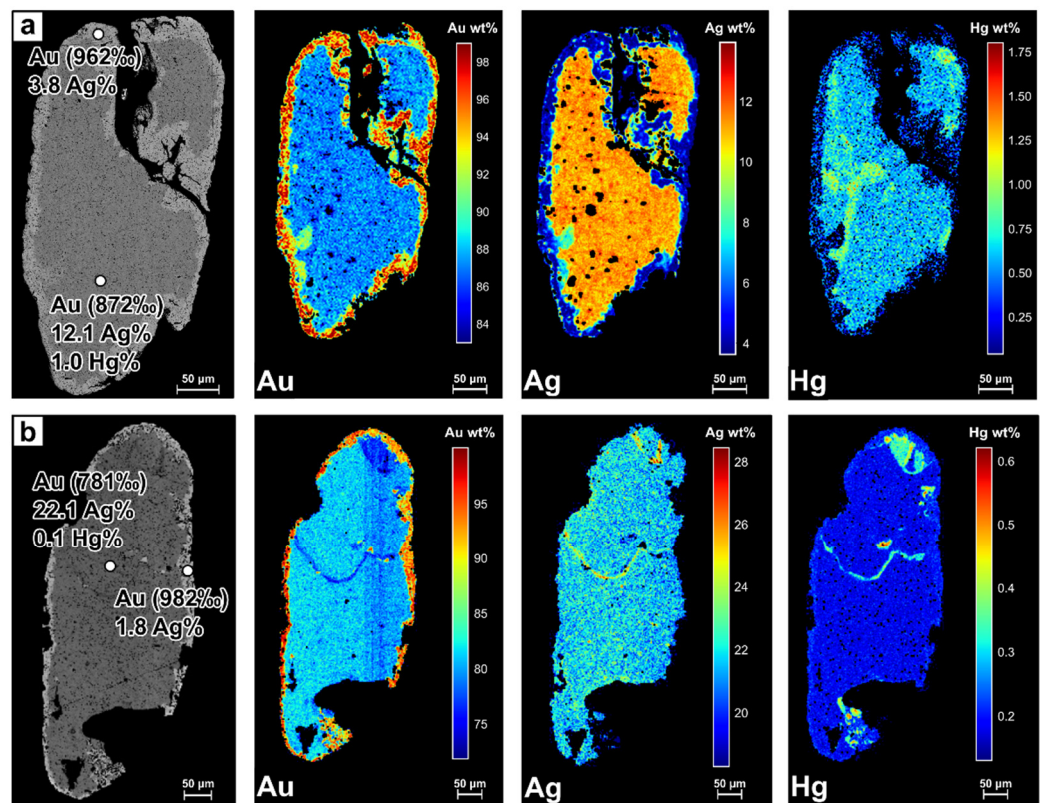


**Figure 6.** BSE image and EMPA chemical maps for Au-Ag-Hg. Colorscale in chemical maps shows the relative element abundance. Composition and native gold fineness in both core and rim of particle are shown. (a) Rim zonation that exhibits Ag-Hg depleted and Au enriched domains toward the edges. There is a sharp contact between the rim and the core. Hg contents seems to be less associated with Au-Ag contents in the particle core (b) Particle showing a compositional heterogeneity in the form of a ‘vein-like’ zone with higher contents of Ag and Hg. In both particles, Hg is absent in particle rims.

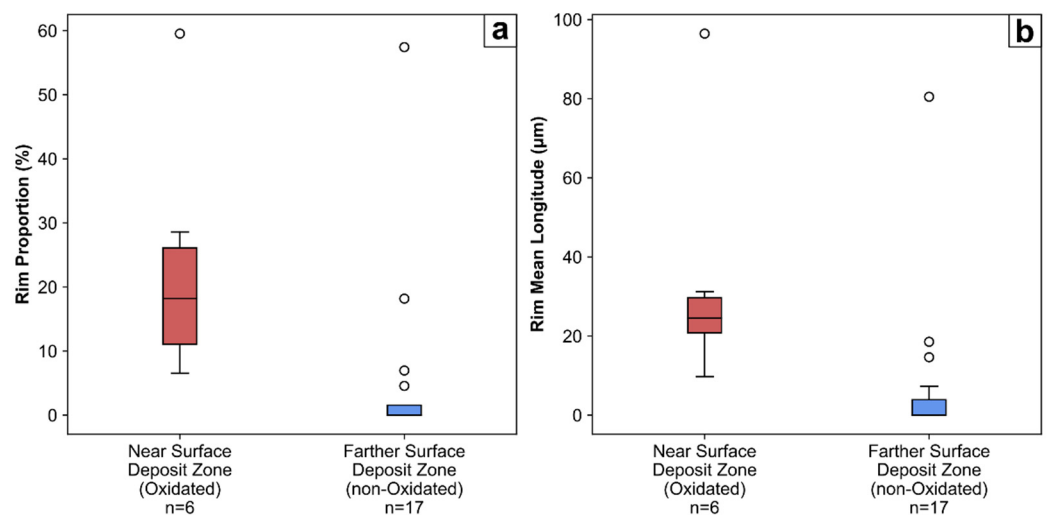


**Figure 7.** Differences in Ag-Hg depleted rim zonation size observed in different zones of the deposits. (a) Proportion of the particle cross-section affected by rim development. (b) Mean longitude of the rim. Near surface zones of the deposit (most oxidated), exhibit a higher rim development than the farther surface zones (non-oxidated).

#### 4.2.2. Mineral Inclusions

Mineral inclusions are a very common feature observed in the Pureo gold particles. Fifty-five of the 75 particles studied using optical microscopy and SEM showed mineral inclusions, mainly composed of silicates and ore minerals. Micron-scaled ore mineral inclusions (Figure 8) were recorded in 29 particles from all mines. The ore minerals identified in SEM with EDS were mainly sulfides such as pyrite, galena and, less commonly, arsenopyrite, chalcopyrite, sphalerite, gersdorffite and Sb-bearing sulfosalts as boulangerite and tetrahedrite. Quartz was the most common silicate. A summary of the ore mineral inclusions and their frequencies can be found in Table 1. These minerals are mainly found as hosted inclusions within particle cores, but in some cases, they occur on particle surfaces (Figure 8b).

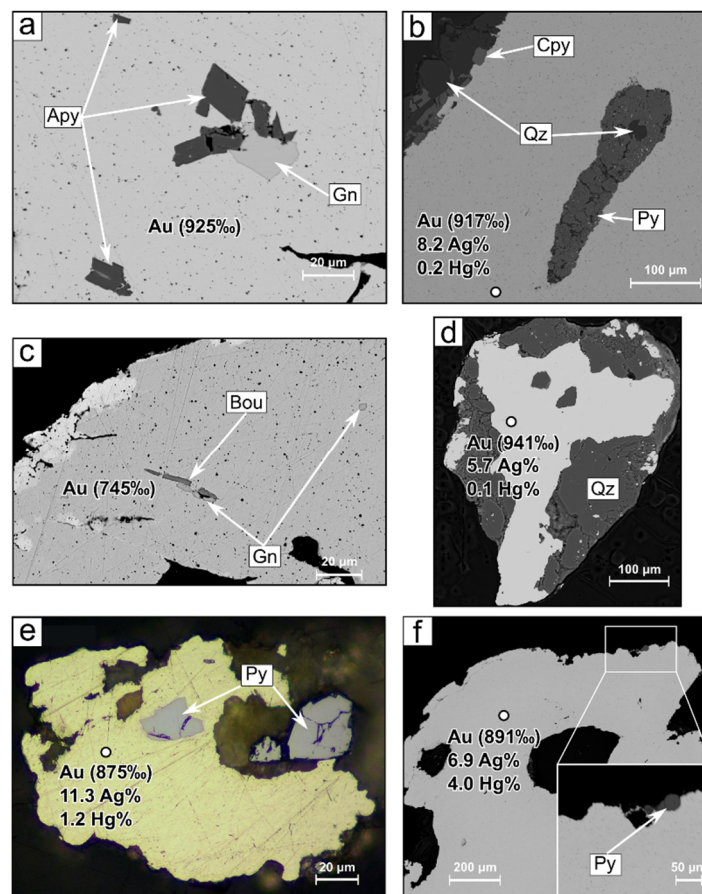


**Figure 8.** BSE and reflected light microscopy images of mineral inclusions in contact with native gold in Pureo particles. Composition and fineness of the hosting native gold is shown. (a) Arsenopyrite (Apy) and galena (Gn) in the particle core. (b) Pyrite (Py), chalcopyrite (Cpy) and quartz intergrowths occurring both in core and surface (upper left corner). (c) Boulangerite (Bou) and galena (Gn) in particle core. A change in the host native gold composition (rim) is visible as a lighter grey zone in the upper left particle border. (d) Quartz present in both core and surface of the particle. (e,f) Pyrite (Py) inclusions in contact with native gold cores with >1 Hg wt%.

The type of ore mineral found as an inclusion is related to the silver content of its host native gold (Figure 9), indicating that certain ore minerals tend to be more common in a determined composition. This relation confirmed the presence of two populations of native gold, as already evidenced with the slope break in silver cumulative frequency curves (Figure 5a). Pyrite, galena, and chalcopyrite are commonly found in low silver particles (lower than 15 Ag wt%; 850‰ Au), whereas arsenopyrite seems to be more frequent in high silver particles (higher than 15 Ag wt%; 850‰ Au). Also, gersdorffite was only observed in

low silver particles, while Sb-bearing sulfosalts as tetrahedrite and boulangerite were only observed in high silver particles.

**Table 1.** Ore minerals found as inclusions in native gold particles.

Placer Location	Total Particles Analyzed	Particles with Ore Mineral Inclusions	Ore Mineral Inclusions
La Familia	8	6	Py, Gn, Apy, Cpy, Gdf
Juanito	36	11	Py, Gn, Cpy, Gdf
Potrerito	26	11	Py, Gn, Sp, Apy, Cpy, Tth, Blg
Curanilahue	6	1	Py, Apy, Gn

Number of particles analyzed and particles with mineral inclusions are shown. Ore mineral inclusions are listed in order of abundance. Mineral abbreviations: Py–Pyrite, Gn–Galena, Apy–Arsenopyrite, Cpy–Chalcopyrite, Sp–Sphalerite, Gdf–Gersdorffite, Tth–Tetrahedrite, Blg–Boulangerite.

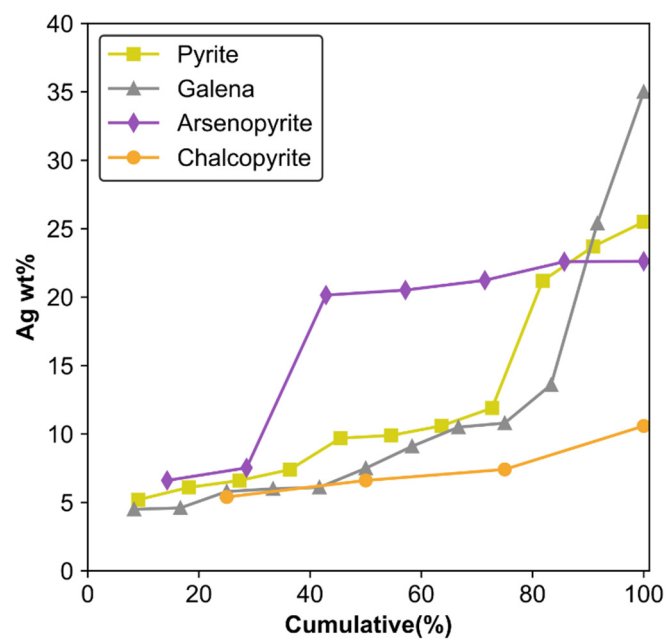


**Figure 9.** SEM-EDS silver contents in native gold particle cores hosting most commonly observed ore mineral inclusions. Arsenopyrite appears to be more abundant in high-silver–low fineness (>15 Ag wt%) particles, while galena, pyrite and chalcopyrite are more likely to be found in low-silver–high fineness (<15 Ag wt%) particles.

## 5. Discussion

### 5.1. Particle Morphology and Transport Distance

The morphological features of placer gold particles are related to their distance of transport [2,3]. One of the main relationships between morphology and transport is particle flatness, which increases with the transport distance, due to progressive particle hammering that occurs during transport [5]. Pureo gold particles show CFI values lower than 6 (Figure 3d), suggesting low transport distances [2,3,5]. CFI values of 1–8.6 would indicate transport distances lower than 1 km [3], a range similar to the one observed in Pureo gold particles. SFI represents the same as CFI, and it has been used by other authors [2,34] to compile flatness and transport distance of placer gold particles in a variety of localities worldwide. These compilations constrain SFI values obtained in Pureo particles to transport distances no further than 15 km. Similarly, HSE values obtained in the particles also point to reduced transport distances, based on the HSE–distance model developed by [30] for Klondike placers. An estimation of transport distance using this model was done with HSE distribution for each mine and weighted according to the number of samples recovered in each mine. Equations and detailed description of the model can be found in [30,36]. The given transport distances for Pureo gold particles are only first-order estimations,

since specific sedimentologic and hydrologic variables for Pureo area placer deposits are unknown. This estimation leads to transport distances between 1–8 km (Figure 10), which is consistent with those estimated with CFI and SFI. As shown with this estimation, transport distances between mines are slightly dissimilar (Figure 10), as Potrerito gold particles shows the lowest CFI, SFI and highest HSE (Figure 3d–f) values, suggesting that these particles have the lowest transport distances (Figure 10). The Curanilahue and La Familia mines show the highest transport distances (Figure 10).

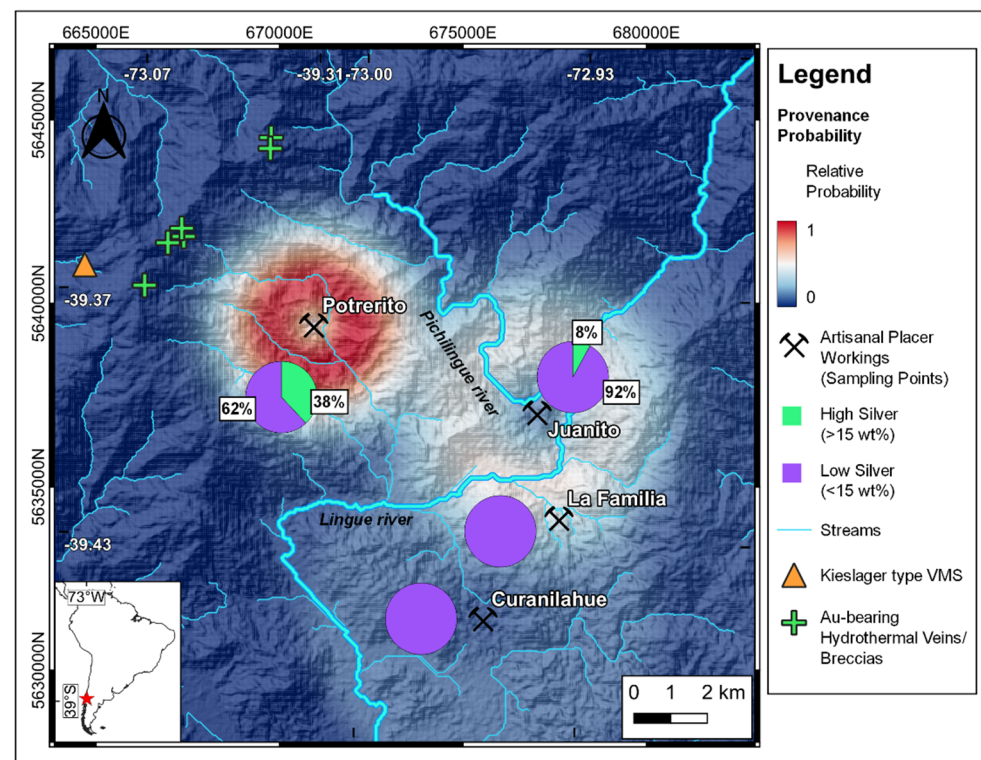


**Figure 10.** Relative probability (values normalized between 0–1) of provenance according to particle morphology quantified by HSE distributions and distance estimated using [30] shape–distance models for Klondike placers. Probability was weighted with the number of samples recovered in each site and normalized, obtaining a relative probability. Proportions of compositional sub-populations occurring in the placers and hypogene mineralizations are shown.

Low transport distances indicated by morphological indices are consistent with the frequent observation of accessory minerals such as quartz or pyrite in particle surfaces, since these are considered inherited characteristics from their primary sources [40]. According to [3], these features are removed rapidly, i.e., in the first hundreds of meters of transport, due to mechanical effects and the chemical instability of minerals like pyrite in the supergene environment. Thus, our results regarding the morphological features of the Pureo gold particles constrain their transport to distances no further than 15 km, indicating a local origin of the gold in the Coastal Cordillera. Our results are consistent with those presented in previous works [10,11] that reported morphological results compatible with low transport distances and a local origin of gold in BMMC rocks in other placer localities in the Coastal Cordillera, such as Marilán, Bahía Mansa, Hueyusca and Madre de Dios [10,11].

## 5.2. Microchemistry and Gold Sub-Populations

The co-existence of native gold and mineral inclusions in placer gold particles is considered to be an inherited relict that reflect the formation conditions of primary gold in the source mineralization [6,41]. As previously shown, the silver cumulative curves for particle cores show a marked slope break around 15 Ag wt% (Figure 5a). This break is interpreted as

the contribution of two compositional sub-populations with different ranges in their silver contents that could be derived from different mineralization styles as sources of gold or a single hypogene source that shows internal zoning due to fluid evolution or multiple paragenetic stages with generation of different gold types [7]. However, this slope break is also visible in the distribution of ore mineral inclusions, where pyrite, galena and chalcopyrite appear to be mostly present in low silver particles, while arsenopyrite appears to be mostly present in high silver particles (Figure 9). Slope breaks in cumulative plots integrating the abundances of ore mineral inclusions with their host native gold silver contents, have been used to support the presence of compositionally distinct sub-populations in placer gold that comes from multiple sources [42,43]. In addition to this, mercury contents observed in particle cores (Figure 5b) can be interpreted as an additional discriminant between sub-populations and hypogene sources [7,44], whose variation is consistent with slope breaks of cumulative silver content curves. Moreover, the compositionally homogeneous cores exhibited by low silver particles contrast with the occurrence of compositional core heterogeneities only observed in high silver particles. These heterogeneities are interpreted to reflect changes in the hypogene mineralizing environment conditions [45]. Therefore, our results indicate that two populations of gold particles are present in the Pureo area, probably deriving from different types of primary sources. Considering the Pureo area geologic context and the presence of more than one type of gold-bearing mineralization style [12,13], the possibility of different sources originating the compositional sub-populations is possible. However, the possibility of a single zoned source cannot be completely discarded, due to the lack of details about the known gold mineralization styles in this area.

Considering this distinction between gold sub-populations, it is possible to see some differences in their morphologies (Figure 11). The grain morphologies in high silver particles tend to show restricted and lower CFI, SFI and HSE values than the low silver particles. Considering the above discussion about the morphology of gold particles, the difference in morphological index values could indicate a rather restricted and local origin for the high silver particles. The proportions of each compositional sub-population in the locations shown in Figure 10 could implicate that the contributing source for high silver particles is restricted to the N-NW of the study area, explaining the absence of those particles in the Curanilahue and La Familia mines (Figure 10).

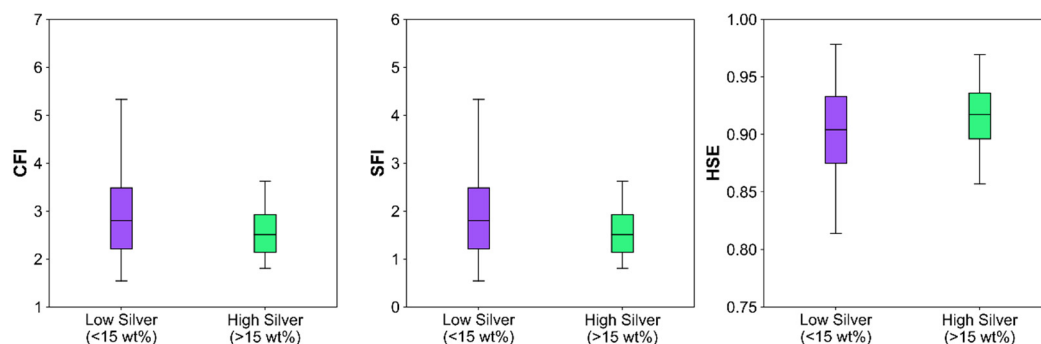


**Figure 11.** Morphological index variations for the two compositional sub-populations. Low silver population shows a broader range of values and higher maximum values than high silver particles, exhibiting possible differences in their transport. CFI: Cailleux's flatness index, SFI: Shilo's flatness index, HSE: Hofmann's shape entropy.

Other features related with supergene environment processes, such as compositional rim formation, were commonly observed in the Pureo gold particles. Rims are a common feature in placer gold particles in a variety of geological environments; their formation is mostly attributed to the removal of Ag and Hg from the native gold, causing a relative enrichment in Au in the particle rim due to exposure to supergene conditions [2,38,39,46,47]. Rims can also be formed due to the authigenic re-precipitation of gold in a supergene environment, a process that can be important in tropical environments [6,48]. Despite this,

the climatic conditions and active tectonics in southern Chile Coastal Cordillera (38° S) do not favor the formation of well-developed weathering fronts as they do in tropical environments [49]. Therefore, this process, although present, may not be so relevant in here. According to [2], the formation of rims in placer gold particles can occur during their transport. Transport is an intermittent process where, for some periods, particles are moving in an active stream while in others, they remain in dormant sediments [2]. Rims are thought to thicken during the latter stages, because as particles move, these rims are removed due to abrasion [2]. In consideration of this, rim formation in the Pureo gold particles was not associated with transport, but rather, with the post-depositional stage of the deposits. Indeed, the differences in the rim development were probably related to their different oxidation levels and the distance to the surface (Figure 7), because oxidation is a key factor in the destabilization of Au-Ag alloys that causes rim formation [39]. In other words, rims in particles extracted from zones of the deposits far away from the surface can be associated with their last exposition to atmospheric conditions before burial, while rims in particles from near surface zones undergo further development and are probably enhanced by the progressive oxidation in these zones.

### *5.3. Mineralization Styles in the Coastal Cordillera and Possible Sources of Gold*

Considering that our morphological data suggest a local origin of gold in the Coastal Cordillera metamorphic rocks, we discuss the possible relationship between placer gold and known primary gold occurrences in these metamorphic rocks.

The nearest possible gold source is the Kieselager VMS mineralization, located at the west of the study area (Figure 1), which corresponds to orebodies composed of pyrite, chalcopyrite, pyrrhothite and minor sphalerite, where minor gold has been described [12,22] as well as the associated exhalites. This is supported by the fact that “coticule” clasts in gravel deposits are present in the host placer deposits, and that these coticules are considered parts of a single VMS sub-marine hydrothermal system which was active during the Paleozoic era and is preserved in the BMMC rocks [12,18,21,23]. Moreover, our results show that the microchemical characteristics of a native gold grain found in a coticule clast [20] are similar to those in the low silver population defined above, with detectable contents of Hg in the native gold (Figure 5b). The formation of Au-Ag-Hg alloys in VMS deposits that have undergone regional metamorphism in similar conditions as the BMMC rocks is reported by [50], suggesting that although these alloys can be formed in the submarine hydrothermal stage of the protolith, they can also form during their metamorphism due to metal remobilization and re-precipitation from other minerals which are present in VMS deposits. Similarly, it has been suggested that hydrated, low to medium grade metamorphism and deformation can promote the growth of pre-existent electrum grains in VMS due to metal remobilization from sulfides [51]. Specifically, gold is known to form from sulfides as pyrite [51] by processes enhancing metal remobilization, as syn-tectonic recrystallization and cataclastic fracturing, features reported in pyrites of the Pirén Alto VMS from the BMMC [20,22]. This suggests that gold possibly formed in pyrite and sulfides from the VMS and surrounding rocks (e.g., ‘coticules’), due to remobilization and re-precipitation during subduction and accretion metamorphism [20]. The above could point to VMS as a contributor for the low silver compositional population. Additionally, the presence of galena, pyrite and chalcopyrite as mineral inclusions in this compositional population, is compatible with an origin in VMS, as these sulfides are common in these deposits and have been described in the local occurrences of VMS in BMMC [21,22]. Although Pirén Alto is the only orebody of this type described near the Pureo area, these occurrences are common in the metamorphic rocks of Coastal Cordillera, with several similar orebodies recognized to the north of the study area [18,21], therefore it cannot be ruled out that more orebodies of similar characteristics have been eroded away in the area or remain undiscovered, contributing to the gold in Pureo placers.

On the other hand, veins and breccias related to hydrothermal activity in Cenozoic intrusions in the BMMC are considered as another possible contributor [12]. The nearest

occurrence of this type of system (Pirén Alto prospect), located around 10 km northwest from the Pureo placers (Figure 1), is characterized by veins and breccias hosted in pelitic and mafic schists of BMMC, with quartz-sericite alteration, where the gold mineralization is associated with pyrite and arsenopyrite [13,25]. This occurrence is probably related to hydrothermal alteration due to felsic sub-volcanic intrusions of unknown age, as observed in drill cores extracted during older explorations of the area [12,24,25]. The association with arsenopyrite in this mineralization style could suggest a relation with the high silver compositional population studied in this work, which is characterized by arsenopyrite abundance as inclusions. However, this relationship is highly uncertain, due to the scarce information of this type of deposits in the Coastal Cordillera. Other possibilities of gold sources from metamorphic rocks of BMMC could be gold-quartz veins found in metamorphic terranes [12]. However, this mineralization style has not been described in BMMC rocks.

## 6. Conclusions

In this study, we analyzed the morphological and microchemical characteristics of gold particles from the Pureo area. Our results allowed us to conclude a low transport distance of gold particles and to identify two compositional sub-populations that could reflect different types of primary sources for gold. The main conclusions of this study are as follows:

1. The morphological characteristics of Pureo gold particles indicate a limited transport, with distances no further than 15 km, probably in the range of 1–8 km, consistent with a local provenance restricted to the metamorphic rocks of the Coastal Cordillera.
2. Particle microchemical characteristics, such as native gold composition and mineral inclusions, allowed us to identify two compositional sub-populations. These compositional types could be associated with two contrasting primary sources, formed by different types of magmatic-hydrothermal and/or metamorphic processes in the Coastal Cordillera. The possible sources of gold can be correlated with two types of hypogene mineralization styles observed in the study area: metamorphosed hydrothermal deposits of the BMMC (metamorphosed Kieslager massive sulfide deposits and their related exhalites) and subsequent magmatic-hydrothermal processes (Cenozoic intrusive activity and related hydrothermal systems).
3. Both characteristics allowed us to conclude a local origin of the gold, restricted to the erosion of rocks present in the Coastal Cordillera. Because some manifestations of possible primary gold source types remain locally and regionally preserved, it is possible that undiscovered deposits exist in this and other regions of the Coastal Cordillera. The microchemical characteristics defined in this work could provide a basis for further exploration works. Therefore, additional work could focus on morphological and microchemical studies of gold particles from other placer deposits in Coastal Cordillera and placers in active rivers.

**Author Contributions:** Conceptualization, P.B. and P.S.-A.; methodology, P.B., B.G. and P.S.-A.; investigation, P.B. and B.G.; resources, J.P. and G.P.; writing—original draft preparation, P.B.; writing—review and editing, P.S.-A., G.P. and J.P.; supervision, P.S.-A. and J.P.; funding acquisition, J.P., G.P. and D.K. All authors have read and agreed to the published version of the manuscript.

**Funding:** This research was funded by FNDR (Fondo Nacional de Desarrollo Regional, Los Ríos, Chile) project “Transferencia Programa de Apoyo a la Pequeña Minería”. Additional support was provided by ANID-FONDECYT Regular grant 1201219 to P.S., ANID-FONDECYT grant 11181048 to J.P. and Amira Global P1249 project grant to J.P.

**Acknowledgments:** We would like to thank the invaluable logistical support and deposit knowledge from gold artisanal miners of Pureo. We thank Emilio Henríquez and SEREMI de Minería de Los Ríos for their administrative and logistic support. We also thank Alexandre Corgne and Jessica Langlade for their support with EMPA analyses. We thank the SEM and TEM technical support of the Electron Microscope Unit, a core facility—Zeiss Reference Center of Universidad Austral de Chile. We thank

Mario Pino for his technical support. Also, we would like to thank Jerson Uribe and Harry Barría for his support during fieldwork.

**Conflicts of Interest:** The authors declare no conflict of interest.

## References

- Boyle, R.W. *Gold: History and Genesis of Deposits*, 1st ed.; Springer: New York, NY, USA, 1987.
- Knight, J.B.; Morison, S.R.; Mortensen, J.K. The Relationship between Placer Gold Particle Shape, Rimming, and Distance of Fluvial Transport as Exemplified by Gold from the Klondike District, Yukon Territory, Canada. *Econ. Geol.* **1999**, *94*, 635–648. [[CrossRef](#)]
- Townley, B.K.; Hérail, G.; Maksaev, V.; Palacios, C.; de Parseval, P.; Sepulveda, F.; Orellana, R.; Rivas, P.; Ulloa, C. Gold Grain Morphology and Composition as an Exploration Tool: Application to Gold Exploration in Covered Areas. *Geochem. Explor. Environ. Anal.* **2003**, *3*, 29–38. [[CrossRef](#)]
- Hérail, G.; Fornari, M.; Viscarra, G.; Miranda, V. Morphological and Chemical Evolution of Gold Grains during the Formation of a Polygenic Fluvial Placer: The Mio-Pleistocene Tipuani Placer Example (Andes, Bolivia). *Chron. Rech. Min.* **1990**, *500*, 41–49.
- Youngson, J.H.; Craw, D. Variation in Placer Style, Gold Morphology, and Gold Particle Behavior down Gravel Bed-Load Rivers; an Example from the Shotover/Arrow-Kawarau-Clutha River System, Otago, New Zealand. *Econ. Geol.* **1999**, *94*, 615–633. [[CrossRef](#)]
- Chapman, R.; Leake, B.; Styles, M. Microchemical Characterization of Alluvial Gold Grains as an Exploration Tool. *Gold Bull.* **2002**, *35*, 53–65. [[CrossRef](#)]
- Chapman, R.J.; Banks, D.A.; Styles, M.T.; Walshaw, R.D.; Piazzolo, S.; Morgan, D.J.; Grimshaw, M.R.; Spence-Jones, C.P.; Matthews, T.J.; Borovinskaya, O. Chemical and Physical Heterogeneity within Native Gold: Implications for the Design of Gold Particle Studies. *Miner. Depos.* **2021**, *56*, 1563–1588. [[CrossRef](#)]
- Chapman, R.J.; Leake, R.C.; Bond, D.P.G.; Stedra, V.; Fairgrieve, B. Chemical and Mineralogical Signatures of Gold Formed in Oxidizing Chloride Hydrothermal Systems and Their Significance within Populations of Placer Gold Grains Collected during Reconnaissance. *Econ. Geol.* **2009**, *104*, 563–585. [[CrossRef](#)]
- Rivera, G. *Entre Circas y Cañuelas: Historia de Los Pirquineros Auríferos de Mariquina, Siglos XVI al XXI*, 1st ed.; San José de la Mariquina, Valdivia, Chile, 2017. Available online: [https://http://2016.literaturalosrios.cl/catalogo/r1112/entre\\_circas\\_y\\_caueelas\\_historia\\_de\\_los\\_pirquineros\\_auriferos\\_de\\_mariquina\\_siglos\\_xvi\\_al\\_xxi](https://http://2016.literaturalosrios.cl/catalogo/r1112/entre_circas_y_caueelas_historia_de_los_pirquineros_auriferos_de_mariquina_siglos_xvi_al_xxi) (accessed on 6 September 2022).
- Ordoñez, A. Oro detrítico en la región de Los Lagos (39–42° S): Mecanismos de transporte y proveniencia. *Serv. Natl. Geol. Miner. (Boletín)* **2000**, *56*, 1–40.
- Zuccone, A. Los placeres auríferos de Madre de Dios y el ambiente metamórfico circundante. Bachelor's Thesis, Universidad de Chile, Santiago, Chile, 1988.
- Muñoz, V. El Basamento Metamórfico Paleozoico, Serie Occidental en la Hoja Queule, IX y X Región, Chile. Condiciones Presión-Temperatura del Metamorfismo. Master's Thesis, Universidad de Chile, Santiago, Chile, 2007.
- SERNAGEOMIN. *Estudio Geológico-Económico de la X Región Norte, Chile*; Servicio Nacional de Geología y Minería: Santiago, Chile, 1998; pp. 1–158.
- Duhart, P.; McDonough, M.; Muñoz, J.; Martin, M.; Villeneuve, M. El Complejo Metamórfico Bahía Mansa en la cordillera de la Costa del centro-sur de Chile (39°30'–42°00' S): Geocronología K-Ar, 40Ar/39Ar y U-Pb e implicancias en la evolución del margen sur-occidental de Gondwana. *Rev. Geol. Chile* **2001**, *28*, 179–208. [[CrossRef](#)]
- Glodny, J.; Lohrmann, J.; Echtler, H.; Gräfe, K.; Seifert, W.; Collao, S.; Figueroa, O. Internal Dynamics of a Paleoacretionary Wedge: Insights from Combined Isotope Tectonochronology and Sandbox Modelling of the South-Central Chilean Forearc. *Earth Planet. Sci. Lett.* **2005**, *231*, 23–39. [[CrossRef](#)]
- Quiroz, D.; Duhart, P.; Crignola, P. Geología del área Lanco-Loncoche, regiones de La Araucanía y de Los Ríos, escala 1:100.000, Carta Geológica de Chile, Serie Geología Básica 106. *Serv. Natl. Geol. Miner.* **2007**, *106*, 1–21.
- Godoy, E.; Kato, T. Late Paleozoic Serpentinities and Mafic Schists from the Coast Range Accretionary Complex, Central Chile: Their Relation to Aeromagnetic Anomalies. *Geol. Rundsch.* **1990**, *79*, 121–130. [[CrossRef](#)]
- Collao, S.; Alfaro, G. Mineralización sulfurada de hierro, cobre y zinc en la Cordillera de la Costa, sur de Chile. *Rev. Geol. Chile* **1982**, *15*, 41–47.
- Quiroz, D.; Duhart, P. Geología del área Queule-Toltén, regiones de La Araucanía y de Los Ríos, escala 1:100.000, Carta Geológica de Chile, Serie Geología Básica 110. *Serv. Natl. Geol. Miner.* **2008**, *110*, 1–22.
- Garroz, B. Estudio del Basamento Metamórfico e Identificación de las Principales Fuentes de oro de los Placeres de Mariquina, región de Los Ríos, Chile. Bachelor's Thesis, Universidad Austral de Chile, Valdivia, Chile, 2022.
- Collao, S.; Alfaro, G.; Hayashi, K. Banded Iron Formation and Massive Sulfide Orebodies, South-Central Chile: Geologic and Isotopic Aspects. In *Stratabound Ore Deposits in the Andes*; Fontboté, L., Amstutz, G.C., Cardozo, M., Cedillo, E., Frutos, J., Eds.; Springer: Berlin, Heidelberg, 1990; pp. 209–219.
- Schira, W.; Amstutz, G.C.; Fontboté, L. The Pirén Alto Cu-(Zn) Massive Sulfide Occurrence in South-Central Chile—A Kieslager-Type Mineralization in a Paleozoic Ensialic Mature Marginal Basin Setting. In *Stratabound Ore Deposits in the Andes*; Fontboté, L., Amstutz, G.C., Cardozo, M., Cedillo, E., Frutos, J., Eds.; Springer: Berlin, Heidelberg, 1990; pp. 229–251.

23. Willner, A.P.; Pawlig, S.; Massonne, H.-J.; Herve, F. Metamorphic Evolution of Spessartine Quartzites (Coticules) in the High-Pressure, Low-Temperature Complex at Bahia Mansa, Coastal Cordillera of South-Central Chile. *Can. Mineral.* **2001**, *39*, 1547–1569. [[CrossRef](#)]
24. Avila, A. *Proyecto Piren, Informe de Avance. Inedit Report*; Minerale Sierra Morena S.A.: Valdivia, Chile, 1990.
25. Troncoso, R.; Cisternas, M.E.; Alfaro, G.; Vukasovic, V. Antecedentes sobre volcanismo terciario, cordillera de la costa, X Región, Chile. In Proceedings of the VII Congreso Geológico Chileno, Concepción, Chile, 17–21 October 1994; Volume 1, pp. 205–209.
26. Duhart, P.; Antinao, J.L.; Clayton, J.; Elgueta, S.; Crignola, P.; McDonough, M. Geología del área Los Lagos-Malalhue, escala 1:100.000, Carta Geológica de Chile, Serie Geología Básica 81. *Serv. Natl. Geol. Miner.* **2003**, *81*, 1–30.
27. Yeend, W.E. *Gold in Placer Deposits*; US Government Printing Office: Washington, DC, USA, 1990; p. 19.
28. Peebles, F. *Estudio Preliminar de las Pertenencias Mineras en los Sectores Madre de Dios y El Roble, Provincia de Valdivia*; Instituto de Investigaciones Geológicas: Santiago, Chile, 1976; pp. 1–8.
29. Agnerian, H. *Report on Madre de Dios Placer Gold Project, Chile. Internal Report*; Global Gold Company: Berlin, Germany, 2007; pp. 1–52.
30. Crawford, E.C.; Mortensen, J.K. An ImageJ Plugin for the Rapid Morphological Characterization of Separated Particles and an Initial Application to Placer Gold Analysis. *Comput. Geosci.* **2009**, *35*, 347–359. [[CrossRef](#)]
31. Schindelin, J.; Arganda-Carreras, I.; Frise, E.; Kaynig, V.; Longair, M.; Pietzsch, T.; Preibisch, S.; Rueden, C.; Saalfeld, S.; Schmid, B.; et al. Fiji: An Open-Source Platform for Biological-Image Analysis. *Nat. Methods* **2012**, *9*, 676–682. [[CrossRef](#)]
32. Cailleux, A.; Tricart, J. *Initiation à l'étude Des Sables et Des Galets*, 1st ed.; Centre de la Documentation Universitaire: Paris, France, 1959; Volume 1.
33. Shilo, N.A.; Shumilov, Y.V. New Experimental Data on Settling of Gold Particles in Water. *Dokl. Akad. Nauk SSR (Earth Sci. Sect.)* **1970**, *195*, 184–187.
34. dos Santos Alves, K.; Barrios Sánchez, S.; Gómez Barreiro, J.; Merinero Palomares, R.; Compañía Prieto, J.M. Morphological and Compositional Analysis of Alluvial Gold: The Fresnedoso Gold Placer (Spain). *Ore Geol. Rev.* **2020**, *121*, 103489. [[CrossRef](#)]
35. Hofmann, H.J. Grain-Shape Indices and Isometric Graphs. *J. Sediment. Res.* **1994**, *A64*, 916–920. [[CrossRef](#)]
36. Crawford, E.C. *Klondike Placer Gold: New Tools for Examining Morphology, Composition and Crystallinity*. Master's Thesis, University of British Columbia, Vancouver, BC, Canada, 2007.
37. Wrighton, T.M. *Placer Gold Microchemical Characterization And Shape Analysis Applied As An Exploration Tool In Western Yukon*. Master's Thesis, University of British Columbia, Vancouver, BC, Canada, 2013.
38. Groen, J.C.; Craig, J.R.; Rimstidt, J.D. Gold-Rich Rim Formation on Electrum Grains in Placers. *Can. Mineral.* **1990**, *28*, 207–228.
39. Krupp, R.E.; Weiser, T. On the Stability of Gold-Silver Alloys in the Weathering Environment. *Miner. Depos.* **1992**, *27*, 268–275. [[CrossRef](#)]
40. Chapman, R.J.; Mortensen, J.K. Application of Microchemical Characterization of Placer Gold Grains to Exploration for Epithermal Gold Mineralization in Regions of Poor Exposure. *J. Geochem. Explor.* **2006**, *91*, 1–26. [[CrossRef](#)]
41. Leake, R.C.; Chapman, R.J.; Bland, D.J.; Stone, P.; Cameron, D.G.; Styles, M.T. The Origin of Alluvial Gold in the Leadhills Area of Scotland: Evidence from Interpretation of Internal Chemical Characteristics. *J. Geochem. Explor.* **1998**, *63*, 7–36. [[CrossRef](#)]
42. Chapman, R.J.; Leake, R.C.; Moles, N.R. The Use of Microchemical Analysis of Alluvial Gold Grains in Mineral Exploration: Experiences in Britain and Ireland. *J. Geochem. Explor.* **2000**, *71*, 241–268. [[CrossRef](#)]
43. Potter, M.; Styles, M.T. *Gold Characterisation as a Guide to Bedrock Sources for the Estero Hondo Alluvial Gold Mine, Western Ecuador. Appl. Earth Sci.* **2003**, *112*, 297–304. [[CrossRef](#)]
44. Mackenzie, D.J.; Craw, D. The Mercury and Silver Contents of Gold in Quartz Vein Deposits, Otago Schist, New Zealand. *N. Z. J. Geol. Geophys.* **2005**, *48*, 265–278. [[CrossRef](#)]
45. Moles, N.R.; Chapman, R.J. Integration of Detrital Gold Microchemistry, Heavy Mineral Distribution, and Sediment Geochemistry to Clarify Regional Metallogeny in Glaciated Terrains: Application in the Caledonides of Southeast Ireland. *Econ. Geol.* **2019**, *114*, 207–232. [[CrossRef](#)]
46. Wierchowicz, J. Morphology and Chemistry of Placer Gold Grains—Indicators of the Origin of the Placers: An Example from the East Sudetic Foreland, Poland. *Acta Geol. Pol.* **2002**, *52*, 563–576.
47. Butt, C.R.M.; Hough, R.M.; Verrall, M. Gold Nuggets: The inside Story. *Ore Energy Resour. Geol.* **2020**, *4–5*, 100009. [[CrossRef](#)]
48. Nichol, I.; Hale, M.; Fletcher, W.K. Drainage Geochemistry in Gold Exploration. In *Drainage Geochemistry*; Hale, M., Plant, J.A., Eds.; Handbook of Exploration Geochemistry; Elsevier: Amsterdam, The Netherlands, 1994; Volume 6, pp. 499–557. ISBN 978-0-444-81854-6.
49. Rivera, J.; Reich, M.; Schoenberg, R.; González-Jiménez, J.M.; Barra, F.; Aiglsperger, T.; Proenza, J.A.; Carretier, S. Platinum-Group Element and Gold Enrichment in Soils Monitored by Chromium Stable Isotopes during Weathering of Ultramafic Rocks. *Chem. Geol.* **2018**, *499*, 84–99. [[CrossRef](#)]
50. Healy, R.E.; Petruk, W. Petrology of Au-Ag-Hg Alloy and “Invisible” Gold in the Troutlake Massive Sulfide Deposit, Flin Flon, Manitoba. *Can. Mineral.* **1990**, *28*, 189–206.
51. Huston, D.L.; Bottrill, R.S.; Creelman, R.A.; Zaw, K.; Ramsden, T.R.; Rand, S.W.; Gemmel, J.B.; Jablonski, W.; Sie, S.H.; Large, R.R. Geologic and Geochemical Controls on the Mineralogy and Grain Size of Gold-Bearing Phases, Eastern Australian Volcanic-Hosted Massive Sulfide Deposits. *Econ. Geol.* **1992**, *87*, 542–563. [[CrossRef](#)]